RainbowLight: Towards Low Cost Ambient Light Positioning with Mobile Phones

Lingkun Li*
School of Software
Tsinghua University
llk16@mails.tsinghua.edu.cn

Pengjin Xie*
School of Software
Tsinghua University
xpj15@mails.tsinghua.edu.cn

Jiliang Wang
School of Software
Tsinghua University
jiliangwang@tsinghua.edu.cn

ABSTRACT

Visible Light Positioning (VLP) has attracted much research effort recently. Most existing VLP approaches require special designed light or receiver, collecting light information or strict user operation (e.g., horizontally holding mobile phone). This incurs a high deployment, maintenance and usage overhead. We present RainbowLight, a low cost ambient light 3D localization approach easy to deploy in today's buildings. Our key finding is that light through a chip of polarizer and birefringence material produces specific interference and light spectrum at different directions to the chip. We derive a model to characterize the relation for direction, light interference and spectrum. Exploiting the model, RainbowLight calculates the direction to a chip after taking a photo containing the chip. With multiple chips, RainbowLight designs a direction intersection based method to derive the location. We implement RainbowLight and extensively evaluate its performance in various environments. The evaluation results show that RainbowLight achieves an average localization error of 3.3 cm in 2D and 9.6 cm in 3D for light on, and an error of 7.4 cm in 2D and 20.5 cm in 3D for light off scenario in daytime.

CCS CONCEPTS

• **Information systems → Location based services**; • **Networks → Location based services**; **Mobile networks**; • **Human-centered computing → Ubiquitous and mobile computing systems and tools**; • **Computer systems organization → Special purpose systems**;

KEYWORDS

Visible Light Positioning; Indoor Localization; Image Processing

ACM Reference Format:
Lingkun Li, Pengjin Xie, and Jiliang Wang. 2018. RainbowLight: Towards Low Cost Ambient Light Positioning with Mobile Phones. In *The 24th Annual International Conference on Mobile Computing and Networking (MobiCom '18), October 29-November 2, 2018, New Delhi, India.* ACM, New York, NY, USA, 13 pages. https://doi.org/10.1145/3241539.3241545

*Co-primary authors.

MobiCom '18, October 29-November 2, 2018, New Delhi, India

ACM ISBN 978-1-4503-5903-0/18/10…$15.00
https://doi.org/10.1145/3241539.3241545

1 INTRODUCTION

The rapid development of mobile and Internet of things (IoTs) facilitates the development of a smarter world. More and more smart robots and smart devices are used in different places, such as factories, airports and even at home. Indoor localization significantly expands the capability of these devices, and thus it attracts much research effort, e.g., a large collection of RF-based [1–8] positioning approaches are proposed.

Visible Light Positioning (VLP) has recently been shown as a promising approach for indoor localization, owing to its potential of high localization precision with ubiquitous existence of light. The basic idea of VLP is to exploit features and information from received light to derive the relative position to light. For example, many approaches use LED light with a controller [9–16] to modulate required features. Thus a receiver can use the modulated features for localization. Further, instead of using a controller to actively modulate information in light, many approaches [17–24] resort to use intrinsic features of light (frequency of fluorescent) or receiver. Meanwhile, [19, 21–24] use geometrical relationship among lights for localization.

Existing VLP approaches exhibit high accuracy for indoor localization. However, there still exist the following limitations that hinder their application: (1) Special designed LED with controller [9, 16] or receiver with sensors [15, 19]. Such kind of LED/receiver is still not widely used in today's buildings. (2) Pre-collected features for all lights[18, 20]. This introduces a high overhead. It is difficult to ensure the features are stable over time and the system needs to keep

update with all lights. (3) Strict usage requirement. For example, [18] requires to keep the mobile phone horizontally and [17] requires to capture at least 3 lamps in a photo each time. Those limitations incur a high deployment, maintenance and usage overhead.

To address those limitations, we propose RainbowLight, a low cost 3D localization approach which significantly reduces the deployment, maintenance and usage overhead. Our key finding for RainbowLight is that light through a chip containing polarizer and birefringence material will produce different interference pattern and light spectrum at different directions. We go deep into the birefringence principle to analyze the relation among direction, light interference and spectrum, and derive a model to characterize the relation. The model builds the foundation of obtaining the direction to a chip based on the received light spectrum. By calculating directions to multiple chips, we can derive the 3D localization of receiver.

In practical design of RainbowLight, we find that light spectrum is difficult to measure on commercial off-the-shelf (COTS) mobile phones. We use hue values extracted from photo to approximate light spectrum and show its effectiveness. To derive light direction for localization, the theoretical model requires various parameters, e.g., optic parameters and thickness of material, which are difficult to measure in practice. Instead of measuring those parameters, we build a sparse initial mapping between hue value and direction by sampling. Further, we conduct model based interpolation on the sparse initial mapping to derive a fine-grained mapping. Such a sparse sampling only needs to be performed once for the same type of polarizer and birefringence material. After capturing a photo containing multiple chips, we calculate hue values of those chips and directions to them. Finally, we leverage a direction based intersection method to calculate the location.

In our implementation, we use transparent adhesive tape as birefringence material. We make small transparent chips by sticking tape with a thin plastic polarizer. In localization, we only need to place multiple chips to a certain plane (e.g., lamp cover, a glass window) to enable it for 3D localization (see Figure 7). It should be noted that RainbowLight does not actively modulate information in the light, and thus it also works for light off scenario in daytime. We can place chips on wall, table, or other flat surface. This significantly extends the application scenarios.

We evaluate the performance of RainbowLight in different scenarios for different types of light as well as different types of surfaces. The evaluation results show that RainbowLight achieves a high localization accuracy and low cost. It also works well even for light off scenario in daytime.

The contributions of our work are as follows:

- We show that light through polarizer and birefringence material will produce different interference pattern and light spectrum at different directions. We analyze and derive a model to characterize direction, interference and light spectrum as the foundation for 3D localization.
- Based on the model, we propose RainbowLight, a low cost ambient light 3D localization approach with a low deployment, maintenance and usage cost.
- We implement RainbowLight and evaluate its performance through extensive experiments. RainbowLight achieves an average localization error of 3.3 cm in 2D and 9.6 cm in 3D, and an error of 7.4 cm in 2D and 20.5 cm in 3D for light off scenario in daytime.

The organization of the remainder is as follows. Section 2 introduces background of our work. Section 3 presents 3D localization model of RainbowLight. Section 4 and 5 introduce the design and implementation of RainbowLight, respectively. Section 6 presents evaluation results of RainbowLight. Section 7 introduces related work and Section 8 concludes this work.

2 BACKGROUND

2.1 Polarization

Polarization is a feature of transverse wave to specify its oscillation in different directions. Natural light, such as light from lamp, has different oscillations. Polarizer for light is a kind of device that allows light with oscillation direction parallel to its *transmission axis*, and blocks light with oscillation direction perpendicular to its transmission axis. Polarizer is widely used in various applications, *e.g.*, each 3D glasses has two polarizers for two lens with different transmission axes allowing light with different oscillation to pass.

A polarizer with a single transmission axis is called *linear polarizer*. Light is polarized after passing through a polarizer. The polarized light has a oscillation direction parallel with the transmission axis of the polarizer. Denote the angle between the oscillation direction of light and the transmission axis of a polarizer as ϕ, according to Malus's law[25], the intensity of the light that passes through the polarizer, denoted by I_ϕ, is given by

$$I_\phi = I cos^2 \phi, \tag{1}$$

where I is the original intensity of light.

In our daily life, natural light such as light from lamp is usually unpolarized, which means that it has oscillation in any direction. When natural light passes through a linear polarizer, it becomes linearly polarized light, i.e., light with a single oscillation direction.

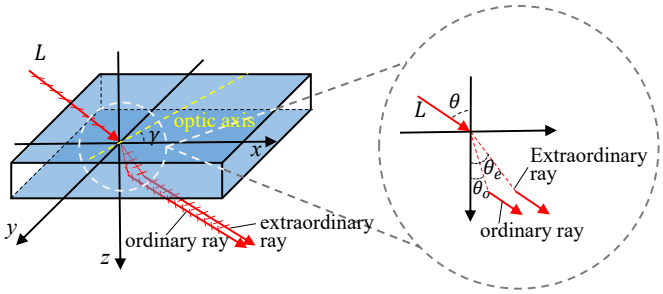

Figure 1: Illustration of birefringence.

2.2 Birefringence

Birefringence is a feature for an optically anisotropic material such as plastics, calcite and quartz. When a ray of light passes through a birefringence material, double refraction can be observed as the light is incident upon the birefringence material. As shown in Figure 1, the ray of light is split into two rays taking different paths in the material. Meanwhile, those two rays have orthogonal polarization directions, and different refractive indices in the birefringence material. There is a special direction, namely *optic axis*, for each certain type of birefringence material. One of the two rays, called *ordinary ray*, has a polarization direction vertical with the optic axis, and the other ray, called *extraordinary ray*, has a polarization direction along the optic axis.

For the ordinary ray, the refractive index is called *ordinary refractive index* and is denoted by n_o. For the extraordinary ray, the refractive index is called *extraordinary refractive index* and is denoted by n_e. Intuitively, a ray of light incident to birefringence material, is split into two rays, i.e., ordinary ray and extraordinary ray. As shown in Figure 1, according to Snell's Law, we have

$$n_{air} sin\theta = n_e sin\theta_e = n_o sin\theta_o \tag{2}$$

where $n_{air} \approx 1$ is the refractive index in air, θ_o and θ_e are the refractive angle of ordinary ray and extraordinary ray, respectively. Usually, $n_e \neq n_o$, and the refractive angles and refractive indexes of ordinary ray and extraordinary ray are different. Thus there is an optical path difference between the two rays after the birefringence material. For a certain type of material, n_o is fixed determined by the material, while n_e varies depending on the direction of the incident ray. As shown in Figure 1, denote the incident angle as θ and the angle between the incident light projection on the incident plane and optic axis as γ. We will show how to obtain n_e and θ_e using θ and γ in practice. Then we can calculate the optical path for ordinary ray and extraordinary ray.

If the incident light L is linearly polarized and the angle between polarization direction and optic axis is ϕ_1, the intensity of ordinary ray I_o and extraordinary ray I_e can be calculated as

$$\begin{aligned} I_o &= I \sin^2 \phi_1 \\ I_e &= I \cos^2 \phi_1. \end{aligned} \tag{3}$$

where I is the intensity of L.

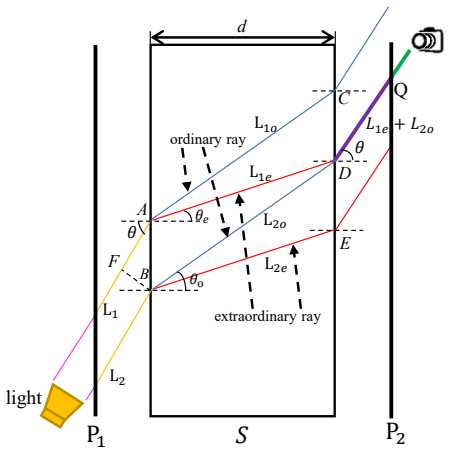

Figure 2: Illustration of light interference.

2.3 Interference

When two light beams L_a and L_b have same frequency, stable phase difference δ and same polarization direction, they can interfere with each other. For different value of δ, the two light beams can have different interference result. The interference intensity can be calculated as:

$$I_i = I_a + I_b + 2\sqrt{I_a I_b} cos\delta \tag{4}$$

where I_i is the light intensity after interference, I_a and I_b are intensity of L_a and L_b, and δ is phase difference between L_a and L_b.

3 LOCALIZATION BASICS

In this section, we show the basic principles of 3D localization for our approach.

As shown in Figure 2, a birefringence material S is placed between two polarizers P_1 and P_2. Light from a source (e.g., a lamp) first passes through polarizer P_1 and becomes a linearly polarized light. Consider two rays of the polarized light L_1 and L_2 incident into S at point A and B, respectively. As introduced in Section 2, L_1 is separated into two parts: L_{1o} (the ordinary ray) and L_{1e} (the extraordinary ray). The refractive indices of the ordinary ray and the extraordinary ray are n_o and n_e, respectively. Similarly, L_2 is separated into two parts: L_{2o} (the ordinary ray) and L_{2e} (the extraordinary ray). After passing through another polarizer P_2, the light L_{1e} and L_{2o} become L'_{1e} and L'_{2o}. L'_{2o} of L_2 interferes with

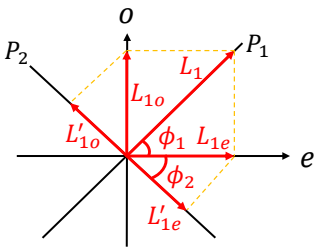

Figure 3: Polarization and intensity change through P_1, S and P_2.

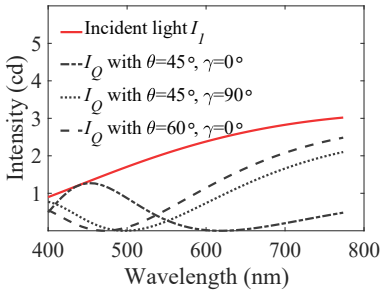

Figure 4: Intensity of interference light for different wavelength with different incident angles.

L'_{1e} of L_1. Then the interference result of light L'_{2o} and L'_{1e} is measured by a camera at Q.

Next in this section, we analyze the light spectrum of interference result and show its relation with the angle θ.

3.1 Interference Analysis

From Eq. (4), we can know that the interference light intensity relies on the two coherent light intensity and their phase difference. We analyze the intensity and phase difference of L'_{1e} and L'_{2o} in the following part.

3.1.1 Intensity. Assume the angle between the optic axis of S and the transmission axis of two polarizers P_1 and P_2 are ϕ_1 and ϕ_2, respectively. As shown in Figure 3, L_1 is the result of light after passing through P_1 and thus its polarization direction is parallel with the transmission axis of P_1. Denote the intensity of L_1 as I_1, and assume light ray L_1 and L_2 have equal intensity. According to Eq. (3), the intensity of $I_{1o} = I_1 \sin^2\phi_1$ and $I_{1e} = I_1 \cos^2\phi_1$.

Denote light intensity of light L'_{1e} and L'_{2o} as I'_{1e} and I'_{2o}. According to Eq. (1), I'_{1e} and I'_{2o} can be calculated as

$$\begin{aligned} I'_{2o} &= I_{1o} sin^2\phi_2 = I_1 sin^2\phi_1 sin^2\phi_2 \\ I'_{1e} &= I_{1e} cos^2\phi_2 = I_1 cos^2\phi_1 cos^2\phi_2. \end{aligned} \tag{5}$$

3.1.2 Phase Difference. As shown in Figure 2, the incident angle of L_1 and L_2 to S are both θ, the thickness of S is d, and the refraction angles of L_{1e} and L_{2o} are θ_e and θ_o. The optical path difference Δ of L_{1e} and L_{2o} at point Q can be calculated as

$$\begin{aligned} \Delta &= \overline{FA} n_{air} + \overline{AD} n_e - \overline{BD} n_o \\ &= d(tan\theta_o - tan\theta_e) sin\theta n_{air} + \frac{d}{cos\theta_e} n_e - \frac{d}{cos\theta_o} n_o \end{aligned} \tag{6}$$

where $\overline{FA}$, $\overline{AD}$ and $\overline{BD}$ are the path length from F to A, from A to D and from B to D, respectively.

Combining Eq. (2) and Eq. (6), we have

$$\Delta = d(n_e cos\theta_e - n_o cos\theta_o) \tag{7}$$

As aforementioned, for a particular material, n_o is usually fixed, n_e and θ_e is related to the incident angle. We put the details of calculating n_e, θ_e and Δ in Appendix A. Therefore, we have

$$\Delta = d(\sqrt{N_e^2 - sin^2\theta(sin^2\gamma + \frac{N_e^2}{N_o^2} cos^2\gamma)} - \sqrt{N_o^2 - sin^2\theta}) \tag{8}$$

where N_o and N_e are principal refractive indices of S, which are fixed given a certain type of material, θ is the incident angle, and γ is the angle between the projection of incident light on the incident plane and optic axis, which is shown in figure 1.

The optical path difference is for two light beams, the phase difference is different for different wavelength. For light with a specific wavelength λ, we can calculate the phase difference δ of L_{1e} and L_{2o} at point D as

$$\delta_D = \Delta \frac{2\pi}{\lambda}. \tag{9}$$

Due to the phase difference of projection on P_2, the phase difference between two coherent lights L'_{1e} and L'_{2o} at point Q is

$$\begin{aligned} \delta &= \delta_D + \delta' \\ &= \begin{cases} \Delta \frac{2\pi}{\lambda} \text{ (case 1)} \\ \Delta \frac{2\pi}{\lambda} + \pi \text{ (case 2)} \end{cases} \end{aligned} \tag{10}$$

where case 1 means the vectors L'_{1o} and L'_{1e} are in the same direction on P_2, and case 2 means they have reverse directions.

3.1.3 Summary. According to Eq. (4), the intensity spectrum of the interference light at Q can be calculated as

$$\begin{aligned} I_Q = {} & I_1 cos^2\phi_1 cos^2\phi_2 + I_1 sin^2\phi_1 sin^2\phi_2 \\ & + 2 I_1 cos\phi_1 cos\phi_2 sin\phi_1 sin\phi_2 cos\delta. \end{aligned} \tag{11}$$

where δ can be calculated according to Eq. (10).

According to Eq. (11), given the intensity spectrum on frequency domain of light source I_1, the angle ϕ_1 between

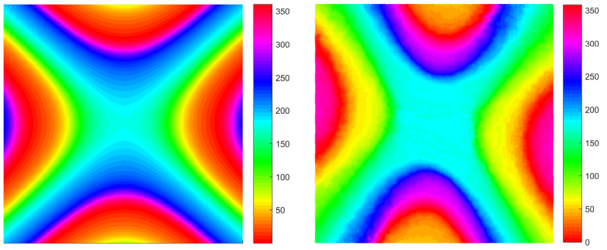

(a) (b)

Figure 5: (a) Hue values on x-y plane by simulation. (b) Hue values measured by mobile phone on x-y plane.

optic axis of the birefringence material and the polarizer P_1, the angle ϕ_2 between optic axis of the birefringence material and the polarizer P_2, the incident direction parameters θ and γ, and birefringence material parameters principal refractive indices and thickness d, we can calculate the value of the light intensity I_Q at Q.

Figure 4 shows the light spectrum of interference for different parameters. Given the value of I_1, ϕ_1, ϕ_2 and d, different combinations of θ and γ result in different spectrum of I_Q. This makes the foundation of obtaining light incident angles information based on different interference result. As long as we can measure the incident angles from multiple points, we can use AoA based method for localization.

3.2 Validation

3.2.1 Choose Light Spectrum Feature. Mobile cameras usually do not have the capability of measuring light spectrum directly. However, the direction information is represented by interference light spectrum, and we have to distinguish different light spectrum to distinguish different directions. There is a challenge for us to find an proper light feature, which satisfies two conditions in the mean time: it can be measured by COTS camera and can indicate the information in light spectrum. It is well-known that different light spectrum can result in different color of the mixed light. A straightforward approach is to measure the RGB color and map RGB vectors to different directions. However, we find this is not feasible in practice as spectrum information cannot be effectively represented in RGB color. Instead, we use the HSL (Hue, Saturation, Lightness) color space and find that the H (i.e., Hue) component from HSL is much more suitable for representing the color of mixtures of lights [26].

3.2.2 Measurement Result. We conduct an experiment to validate the model. We measure the hue value on different positions after P_2. Figure 5b shows the measurement hue values for different positions on a plane with a certain distance to the light. Then we compare the measurement result with

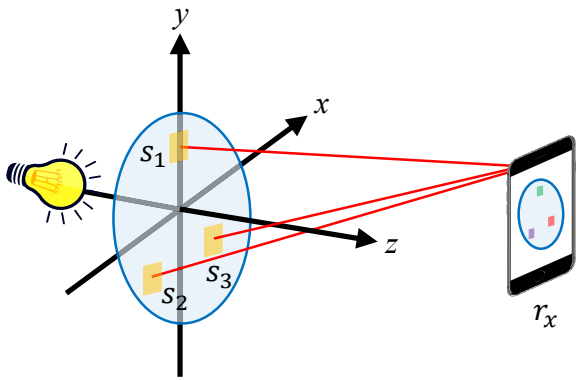

Figure 6: Overview of RainbowLight.

the simulation result based on Eq. (11). In our simulation, we use the parameters of quartz crystal (a birefringence material) chip with thickness of 0.6 mm. We measure the intensity spectrum of interference result on different direction. We leverage the color wheel [26] to approximate intensity spectrum with hue value. Figure 5a shows the hue value with respect to positions on a surface parallel with birefringence chip. We can see that the color regularity in Figure 5a and Figure 5b are very similar. This coincides with our analysis and Eq. (11). This also means that hue value is effective for representing the intensity spectrum.

4 RAINBOWLIGHT DESIGN

4.1 Design Overview

Figure 6 illustrates system overview of RainbowLight. The chips used in RainbowLight are a combination of two polarizers and one birefringence chip as shown in figure 2. With one chip, we can calculate direction information. Combining the direction information from multiple chips, we can can derive the 3D location. The main design of RainbowLight consists of two parts. The first part is mapping initialization. This part is to build an initial mapping between the direction and hue value for a certain type of chip. The mapping initialization only needs to be performed once for a certain type of chip. The second part is the 3D localization component. In this part, a mobile camera will take a photo containing multiple chips. Based on the hue value of the initial mapping, the direction to those chips can be calculated. Then we also propose a direction intersection based method to calculate the final 3D location.

4.2 Mapping Initialization

The mapping between light direction and hue value can be built by sampling on different positions. We put a chip at the origin O of coordinate system, and the chip is parallel with

the x-y plane. A mobile phone moves in a grid at a certain plane ($z = 1m$) and captures a photo containing the chip at each position. For a sampling position r, it derives the hue value h of the color for the chip from the captured photo. It means that the hue values for all points on line $\overrightarrow{Or}$ are h, respectively.

Therefore, we build a mapping $R_S \rightarrow H_S$ from sampling positions $R_S = (r_1, r_2, \ldots, r_n)$ to hue values

$$H_S = \left(\ h_1, h_2, \cdots, h_n \ \right) \tag{12}$$

where h_i denotes the hue value observed by mobile phone from points on line $\overrightarrow{Or_i}$.

For a higher sampling density, the mapping should be more accurate. On the other hand, a higher density also indicates a higher sampling overhead. To reduce the initial sampling overhead, we propose an interpolation based method to improve the granularity of initial mapping. We leverage the color regularity to interpolate a coarse-grained sampling matrix H_S and build a fine-grained mapping $R \rightarrow H$. We examine the performance of interpolation under different sampling density in Section 6.2.

As shown in Figure 5, the color gradually changes with the position. As the hue value ranges from 0 to 360, in interpolation we should carefully deal with the hue value cross the hue range boundary. More specifically, for two hue values h_1 and h_2 ($h_1 > h_2$) for two adjacent sampling positions, we first calculate the hue value gap $h_\Delta = h_1 - h_2$. If h_Δ is smaller than a pre-defined threshold thr (e.g., $thr = 350$), the interpolation can be performed between h_1 and h_2. If h_Δ is larger than the pre-defined threshold thr, we consider the hue value between those two sampling positions cross the hue value boundary. The interpolated hue value should be performed for h_1 and $h_2 + 360$. All the hue value should be calculated from the interpolation result modulus of 360 to guarantee the hue values are in $[0, 360)$.

In practice for the same type of chip, we only need to build initial mapping $R \rightarrow H$ once. This could significantly reduces the initialization overhead for RainbowLight. Later, we will show how to leverage the mapping for localization in 3D space.

4.3 3D Localization

4.3.1 Localization Design. To enable 3D localization, we simply stick several chips on a transparent surface. Without loss of generality, we assume three chips S_1, S_2 and S_3 are used. Later, in Section 6, we will show the impact of number of chips. Denote the position of the center of S_1, S_2, and S_3 as p_1, p_2 and p_3, respectively. The position p_1, p_2 and p_3, namely reference points, can be measured in advance.

A mobile phone with a camera at position r_x simply captures a photo containing S_1, S_2 and S_3. We calculate the hue values $\tilde{h}_1$, $\tilde{h}_2$ and $\tilde{h}_3$ from the photo for those three chips. Based on the initial mapping between color and directions, RainbowLight can obtain the possible directions from p_1, p_2 and p_3, respectively. Thus we have three groups of ray directions from three reference points, respectively. Then we can obtain the position r_x based on the intersection of those ray directions.

4.3.2 Intersection Based Localization. The goal of localization is to calculate the position r_x based on $\tilde{h}_1$, $\tilde{h}_2$ and $\tilde{h}_3$ and $R \rightarrow H$.

Find line group candidates: The initial mapping is built using a chip at coordinate origin O. In practical, chips are usually attached at other positions. In order to make the mapping $R \rightarrow H$ suitable for the deployment of specific chip, we need to do coordinate translation for the initial mapping. The mapping becomes $R^j \rightarrow H$ for $j = 1, 2, 3$, where $R^j = R + p_j$ is the transformed sampling position for S_j.

Due to color error for camera on mobile phone, there may be multiple lines with hue close to $\tilde{h}_1$, $\tilde{h}_2$ and $\tilde{h}_3$. Meanwhile, according to Eq. (11), we also find that there are multiple combinations of θ and γ leading to the same hue value. It indicates that there may be multiple directions of the same hue value. Therefore, for each chip, we can calculate a group of lines. Overall, we obtain three groups of lines denoted by G_1, G_2 and G_3. We have $G_j = \{\overrightarrow{r_i^j p_j} || h_i - \tilde{h}_j| < \epsilon_h\}$ for $j = 1, 2, 3$ where $r_i^j \in R^j$ and ϵ_h is the maximum allowed hue error.

Line intersection: The main idea is to calculate the localization based on the intersection point of those three sets of lines G_1, G_2 and G_3 as the localization result r_x. There should exist three lines from G_1, G_2 and G_3, respectively, that intersect at point r_x. Due to hue value measurement error, those three lines may be very close to each other but not directly intersect in practice. Therefore, we introduce virtual intersection point for two lines. A virtual intersection point exists for two lines when their distance is less than a threshold, and the virtual intersection point can be calculated as the middle point of the shortest line segment between those two lines. Intuitively, only when two lines are close to each other, there exist a virtual point for those two lines.

To find the location of r_x, we need to find the intersecting line triples, i.e., $(\overrightarrow{r_l^1 p_1}, \overrightarrow{r_m^2 p_2}, \overrightarrow{r_n^3 p_3})$ where $\overrightarrow{r_l^1 p_1} \in G_1$, $\overrightarrow{r_m^2 p_2} \in G_2$, $\overrightarrow{r_n^3 p_3} \in G_3$ and $\overrightarrow{r_l^1 p_1}, \overrightarrow{r_m^2 p_2}, \overrightarrow{r_n^3 p_3}$ have pair-wise virtual intersection points. For each line triple, we check the inter-distance between corresponding pair-wise virtual intersection points. If the inter-distance between any pair-wise virtual intersection points is below a threshold ϵ_d, we calculate a candidate location using the center of the triangle defined by those

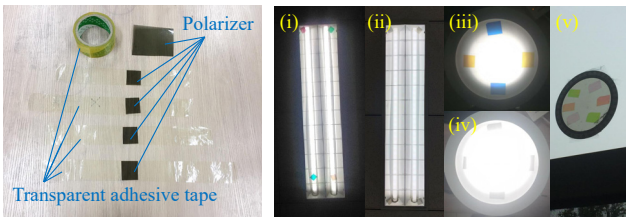

(a) (b)

Figure 7: (a) Chips in RainbowLight (b) anchor with chips made by two polarizers and one transparent adhesive tape (i): near to fluorescent (iii) on LED lamp cover, anchor with chips made by one polarizer and one transparent adhesive tape(ii): near to fluorescent (iv): on LED lamp cover, (v): anchor on a glass window.

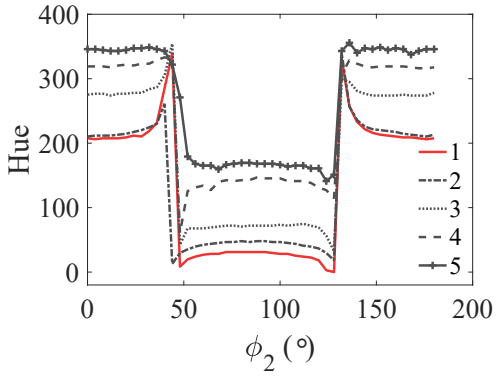

Figure 8: Complementary hue observed as rotating mobile phone for different tape thickness (1 ~ 5).

three virtual intersection points. For each line triple, we calculate a corresponding candidate location. Then we calculate r_x as the average of all candidate locations.

As a summary, the main steps for line based localization algorithm for a mobile phone is as follows:

(1) Captures a photo containing multiple chips.
(2) The mobile phone derives hue values h_x for all the chips from the photo.
(3) Based on h_x and the mapping $R \rightarrow H$, find the line groups from each chip.
(4) Find all line triples that have pair-wise virtual intersection points.
(5) Calculate the candidate points based on the intersection points.
(6) Calculate the final position r_x based on candidate points.

5 IMPLEMENTATION

RainbowLight consists of two components: anchor and receiver. In this section, we present details of those two components. We also discuss a variant of RainbowLight, which put polarizer P_2 in front of the camera in order to eliminate color observed by human eyes. Since RainbowLight performs relative localization for a given anchor, it needs to identify which anchor is captured by camera hence can be used in a large region. We also discuss how to provide identifier to anchors in this section.

5.1 Anchor

The anchor of RainbowLight composed by a group of chips. Each chip consists of two linear polarizers and a thin birefringence material chip. We stick the birefringence material chip between two linear polarizers. As shown in Figure 7a, we use everyday transparent adhesive tape as birefringence material. RainbowLight does not require to stick the anchors on a lamp. We can put anchors different surfaces as long as light can pass through the chips. For example, as shown in figure 7b (i), (iii) and (v), we put anchor near lamps or on lamp cover or on window. As shown in figure 7b(i) and (iii), despite chips display colors, each chip made by polarizers and transparent adhesive tape is very small. It would not disturb human eyes. To enable RainbowLight, we also need to record the relative position for those chips.

5.2 Receiver

We use smartphone as the receiver side. The camera can capture a photo containing the anchor. We implement a software on mobile phone based on Android. After obtaining the photo, we use OpenCV to localize the position of each chip in the image based on features such as shapes, and derive HSL information from the photo. To address hue value estimation error in practice, we use the averaged hue value for each chip as the hue value for localization. To simplify our implementation on localization in mobile phone, we extend our hue values of 2D plane in the initial mapping to hue values in 3D space, as points on the same direction having the same hue value.

In such a case, human eyes cannot observe the color displayed by chips directly as shown in figure 7b (ii) and (iv) , but camera can capture chips with different colors. However, if we put P_2 in front of camera, rotate camera will cause chips color changes, thus color-direction mapping cannot be used. Fortunately, since hue value instead of RGB to represent color in RainbowLight, chips only shows two complementary hue values with camera's rotation as shown in figure 8. Therefore, we measure camera's rotation angle firstly, if it shows complementary hue values of initialization, we can transform to original hue values hence perform localization. Attaching polarizer in front of camera will bring in extra costs, and brings error in accuracy with camera's rotation.

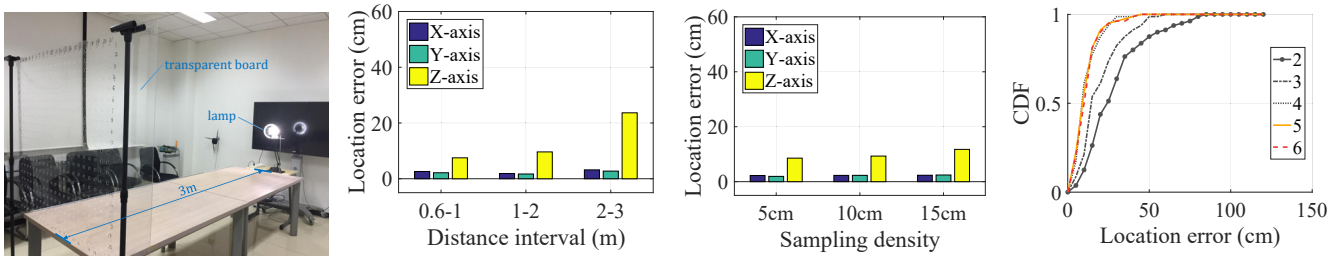

(a) (b) (c) (d)

Figure 9: (a) Experiment environment. (b) Localization precision on different distance. (c) Localization precision on different sampling density. (d) Localization accuracy for different # of chips.

We will present the accuracy in section 6. Users who deploy the RainbowLight can choose where to put the polarizer P_2 according their own conditions and requirements.

As RainbowLight performs localization with camera, power consumption will become a non-trivial issue. We will optimize in the future work by adding scheduling strategy of camera such that camera only open when user needs localization.

We measure the latency of RainbowLigth. In the measurement, we let RainbowLight process 10 photos to measure the average latency. The mobile phone we used is Huawei Nexus 6P. It takes 236 ms in average to find chips and extract hue values. It takes 503 ms in average for 3D localization from hue values. We optimize RainbowLight 3D localization to parallel the processing in our implementation of localization. With such an optimization, the time for 3D localization reduces to 123 ms in average. This should be applicable to most VLP based applications such as navigation.

5.3 Providing Identifier

RainbowLight performs relative localization for a given anchor. To extend RainbowLight to a large area, we need to put more than one anchors in this area. In such a case, RainbowLight needs to identify different anchors.

We can use existing method such as iLAMP [20] to distinguish different lights in a building if we put anchor on the lamp. We also can attach QR code on each anchor to identify them. Considering iLAMP cannot be used with light-off, we also design a QR-code-like method with our chips for providing ID. According to Eq. 10, if we rotate the polarizer P_1 by 90° and fix S and polarizer P_2, the interference result will accordingly change. The frequencies with constructive interference become destructive interference, and vice versa. As a result, the hue value changes to its complementary hue value. We can use this phenomenon to encode identifiers of anchors by using polarizers with different transmission axes. For example, we use a pair of orthogonal polarizers to represent 0 and 1 respectively, leading to two different colors. Then we can use existing encoding method such as matrix code to encode information with those two colors. By using such a method, the chips used in the matrix code can also be used for localization.

6 EVALUATION

We evaluate the performance of RainbowLight from the following aspects:

- Localization accuracy for different distance.
- The impact of system parameters to localization accuracy.
- System performance under different light sources (different manufacturers, color temperature, lamp type and power).
- System performance with light on/off.
- System performance with different mobile phone orientation.

Through the evaluation, we aim to show the effectiveness of RainbowLight in practice. It should be noted that for all experiments we use the same initial mapping unless otherwise specified. This means that we only need to perform initialization once, which significantly reduces the initialization overhead compared with existing approaches.

6.1 Localization Accuracy

Figure 9a shows the experiment environment. In the experiment, we move a transparent board to different distances to the light source. For each distance, we move the mobile phone on the board at different positions. We can measure the position of mobile phone on the board as the ground truth. Meanwhile, we also use RainbowLight to calculate the position of mobile phone. We switch off other lamps during our experiment at night. Figure 9b shows the localization error for mobile phone at different distance. We can see that the localization error increases as distance increases. This is

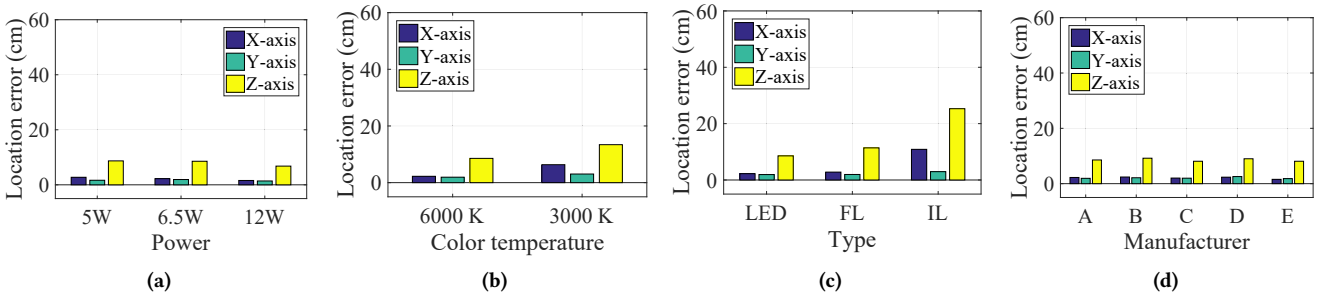

Figure 10: Localization accuracy for different lamps. (a) power, (b) color temperature, (c) types of lamp, (d) manufacturers.

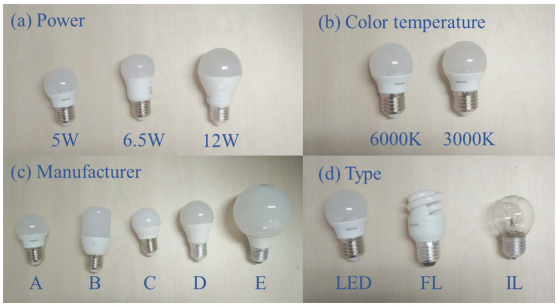

Figure 11: Different light sources.

mainly because hue value is less sensitive with the position for a larger distance.

We can also observe that the error on z-axis is obviously larger than that on x-y plane. The major reason is that the angle from chip to the mobile phone varies by a smaller value when we move the mobile phone along the z-axis than that along the x-y plane. This phenomenon is more evident when chips are close to each other. However, even when those chips are all in a circle with diameter less than 16 cm, the localization accuracy for different distance is still high. This indicates RainbowLight can work for different distance with lamp of small size.

Overall, in the 2 m-3 m distance interval, the mean error of localization is 3.19 cm on x-axis, 2.74 cm on y-axis, and 23.65 cm on z-axis. This performance is better that SmartLight with a localization error of about 60 cm on z-axis for distance from 1 m - 3 m. The localization accuracy of RainbowLight is enough for most today's application scenarios such as navigation.

6.2 Impact of Sampling Density

We examine the impact of sampling density in building initial mapping. Figure 9c shows the localization accuracy with respect to different sampling density. We build the initial mapping on a plane parallel to $x - y$ plane with $z = 100$ cm. We examine the performance with different inter-distance of sampling position, i.e., 5 cm, 10 cm, and 15 cm, respectively. It can be seen that low sampling density still works well for RainbowLight. Even when the inter-distance is 15 cm, the localization error is only around 10 cm. This is mainly because hue value distribution is smooth in the 3D space and thus interpolation is effective in building initial mapping.

6.3 Impact of # of Transparent Chips

As shown in section 4, the hue value from a single chip determines a candidate group of rays from the chip. With more chips, the localization accuracy will be improved as intersection point can be refined with more groups of rays. We explore the relationship between localization accuracy and number of chips. Figure 9d shows the CDF of 3D localization error while increasing the number of chips from 2 to 6. It can be seen that the localization accuracy increases when the number of chips increase from 2 to 4. Further, the performance becomes relatively stable when the number increases from 4 to 6. This means 4 chips is enough in practice to achieve a good localization accuracy.

6.4 Impact of Different Light Source

We examine the performance of RainbowLight with different light sources. As shown in Figure 11, we use lamps of different types, i.e fluorescent (FL), LED and incandescent bulb (IL), from different manufacturers (A - E), with different color temperature (3000 K, 6000 K) and different power (5 W, 6.5 W, 12 W). In all the following experiments, we use a Philips (manufacturer A) 6.5 W LED with color temperature 6000 K for initialization.

In our daily life, the power of LED mainly ranges from 5 W to 20 W. Figure 10a shows localization error of LED (manufacturer A) of power 5 W, 6.5 W and 12W. There is no significant difference in terms of error for different power. This is mainly because as long as γ and θ are fixed, our

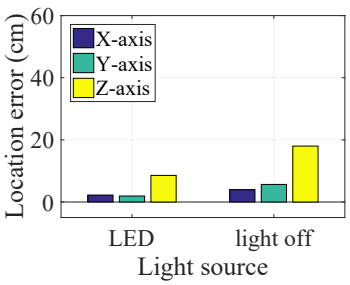

Figure 12: Localization precision of indoor environment with lamp off in daytime.

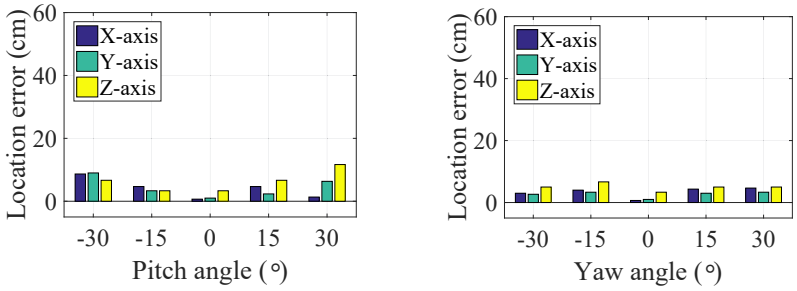

(a) (b)

Figure 13: Localization precision of different (a)pitch and (b)yaw angles of mobile phone.

approach captures the major property of light spectrum and also removes other noise such as brightness, as explained in section 3.

There are mainly two different color temperatures (6000 K and 3000 K) for typical lamps in our daily life. Intuitively, 6000 K generates white color while 3000 K generates yellow. The light spectrums from those two temperatures are slightly different. We initialize with a 6000 K lamp and measure the localization error for 3000 K and 6000 K. As shown in Figure 10b, we can see that the localization error of 3000 K is slightly larger than that of 6000 K because of spectrum difference. However, the accuracy for both color temperature is still acceptable. In practical applications, we only need to build the initial mapping with one color temperature, and RainbowLight performs well under other color temperatures.

We examine the performance of RainbowLight for three most commonly used lamps, i.e. LED, fluorescent and incandescent bulb. As shown in Figure 10c, the accuracy for fluorescent is high. The accuracy of incandescent bulb is relatively low. This is because those two types of lamps have different light spectrum. However, as long as we use incandescent bulb for initialization, the accuracy of RainbowLight remains high.

We also examine the performance of lamps. Light spectrum emitted slightly varies for lamps from different manufactures. We choose 5 LEDs from 5 different popular manufacturers, marked as A-E. The power of all lamps is 5 W. The color temperature is 6000 K. Figure 10d shows that the error is small for all brands and the performance is similar for all brands. It also indicates we only need to initialize with a certain brand, and the accuracy of RainbowLight is acceptable under other brands.

Summary. RainbowLight achieves a high accuracy under different circumstances with commonly used lamps. For most scenarios, RainbowLight only needs to be initialized once, and almost can be used for all other lamps. This significantly reduces the deployment cost and makes RainbowLight practical.

6.5 Localization with Light Off

Most existing visible light positioning systems, e.g., LiTell[18], SmartLight[16] and CELLI[9], only work when light is on, as those systems require modulating information in light or measuring special features from light. This significantly hinders their application in daytime when light is usually switched off. RainbowLight can work even when light is switched off during daytime as it does not need to modulate information in light or measure light features. Figure 12 shows the performance of RainbowLight with light off. Similar to section 6.1, we examine the accuracy in the environment as shown in Fig. 9a. In the experiment, sunlight pass through the window and we switch all lamps off. We can see that the error for light off is still less than 20 cm. The error for light off is very small and is similar to the scenario of light on. This is mainly because RainbowLight can generate obvious features from different light sources, and can also effectively extract those features. This significantly extends the application for visible light based localization and make it more practical in everyday life.

6.6 Impact of Mobile Phone Orientation

To verify influence of pitch and yaw, we measure error at distance 60 cm with different pitch and yaw angle. Figure 13a and Figure 13b shows the result. We select range from -30° to 30° because the mobile cannot capture the lamp with pitch and yaw angle out of this range. We can see that when we change pitch and yaw angle, error changes slightly. This is mainly because when we change the pitch and yaw angle, ϕ_1, ϕ_2, γ, and θ does not change.

If P_2 is attached on the chip, mobile phone roll will have no impact on the hue value. If we put the polarizer P_2 in

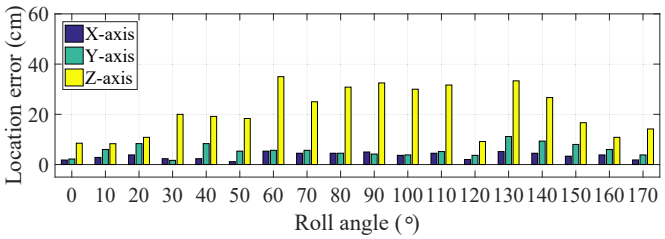

Figure 14: Localization precision of different roll angles of camera

front of camera, RainbowLight needs to confirm if chips on anchor shows complementary hue value and its impact to localization accuracy. We also examine accuracy of localization in this scenario. Error of different roll angles of camera as shown in figure 14.

Therefore, no matter which position we are, as long as we can capture the lamp with any 3D orientation, RainbowLight shows a high localization accuracy. This extends application scenarios of today's VLP systems.

7 RELATED WORK

7.1 Visible Light Based Localization

The first category of work is to use a specially design LED light to generate identifiable features [10–13]. Those works usually need to a use an MCU to control the lamp to modulate information by change the frequency, voltage, etc. Spotlight [14] generates a sequence of on/off pattern and uses such a pattern as landmarks for localization. Spinlight [15] uses a hemispherical shade to encode position information with holes. CELLI [9] designs a structure with LCD to modulate polarization direction of emitting light. It generates two sweeping lines with special light properties and uses sweeping lines for localization.

Recently, SmartLight [16] proposes an interesting idea to use digital modulated LED array with a len to achieve single light 3D localization. It modulates different LED lights with different frequency on the LED array. Then it emits the light through a len to the 3D space. Then it derives the location based on the frequency of received light. Pulsar [19] uses inherent features of photodiode diversity. It builds a map from angle to RSS. It designs a special receiver with two photodiodes. Most of those approaches in this category require a specially designed lamp or receiver. Thus it may not be applicable to most scenarios in our daily life.

Further, many attempts are proposed to remove the requirements with specially controlled light. Existing methods such as [21–24] use geometrical relationship among lights with known position for triangulation based localization. Those methods needs to extract position relationship to those lights from captures photos. PIXEL [17] proposes to leverage inherent feature of optical rotatory dispersion for localization. When a linearly polarized light passes through a disperser, the color observed through a polarizer with different transmission direction should be different at different locations. By fixing a mobile phone orientation, [17] derives the identifier by the observed color, then calculates location with geometrical relationship. It requires to capture more than one light in one photo.

LiTell [18] and iLAMP [20] use inherent features of fluorescent such as frequency and color spectrum to identify each light. Given the position of light, the location can be derived by triangulation. Those two approaches are very nice as they do not need any extra modification to the lamp. However, they require to sample the features for each light. It is also highly related to environment and cannot work when a lamp is changed. Recently, [27] proposes an interesting method of using light to correct inertial measurement unit errors. As introduced in [27], it leverages the property that a polarized light ray going through transparent tape is rotated by an amount related to wavelength. Then it try to derive the location change by sensing the color after a polarizer with different direction. It detects color change by edge crossing between four types of blocks hence serve as landmarks to correct IMU drift errors.

Luxapose [23] localizes the relative position from lamps. The main idea is to build a geometrical model and calculate the position based on relationship between lamps' positions both in the real world and in the photo. It needs to use other extra-information, e.g., focal length or data from other sensors. The model in RainbowLight currently is not based on the relationship between lamp positions. Travi-Navi [28] using computer vision based approach to launch the navigation. It stores guider's video and uses sensors to calibrate the position, and those data can be further used for follower in navigation.

7.2 Other Localization Approaches

Localization has attracted many research efforts. Besides visible light based localization, there exist a large collection of localization approaches using wireless signal, such as [1–8, 29–33], using acoustic signal [34–38], using environment information and cell tower signal [39]. FM signal [40], stride information [41], etc. Those approaches are usually based on a signal attenuation model or pre-collecting a large number of fingerprints. Meanwhile, many wireless signal based approaches need to analyze signal properties such as CSI, which further leads to a high computation overhead. Thus they usually require special designed hardware at the receiver or sender, making it difficult to implement on mobile

phone. Multiple path effect also affects the localization accuracy for many of those approaches. Our approach is largely inspired by those approaches.

8 CONCLUSION

We present RainbowLight, a high-precision 3D visible light based localization system. Compared with existing approaches, RainbowLight does not require special hardware design and pre-collected light features. RainbowLight works on COTS mobile phones without strict user holding requirement. It works well for different types of lamps as well as light off scenario. Those features significantly reduce the deployment, maintenance and using overhead. The evaluation results show that RainbowLight achieves an average localization error of 3.3 cm in 2D and 9.6 cm in 3D. We believe RainbowLight can be applied to today's buildings with a very small overhead to enable many visible light based applications.

ACKNOWLEDGEMENT

We sincerely thank anonymous reviewers and shepherd for insightful comments to improve our work. This work is in part supported by National Natural Science Fund for Excellent Young Scholars (No. 61722210), National Natural Science Fundation of China (No. 61572277, 61532012), and National Key R&D Program of China 2018YFB1004800.

APPENDIX

A. Calculation of n_e, θ_e, and Δ

Inspired by [42], as shown in Figure 1, we let incident point of light as origin, and the projection of incident light to the incident plane as x-axis. We use θ to indicate the incident angle, and θ_o and θ_e are refraction angle of ordinary ray and extraordinary respectively. γ is angle between optic axis and x-axis, i.e. angle between optic axis and projection of incident light.

The directional vector of optical axis, ordinary ray, and extraordinary ray in the birefringence are

$$e_a = (cos\gamma, sin\gamma, 0) \tag{13}$$

$$e_{ko} = (sin\theta_o, 0, cos\theta_o) \tag{14}$$

$$e_{ke} = (sin\theta_e, 0, cos\theta_e) \tag{15}$$

We assume the angle between optic axis and extraordinary ray is α, i.e. angle between e_a and e_{ke}. So according to (13),(15), we have:

$$cos\alpha = e_a \cdot e_{ke} = cos\gamma sin\theta_e \tag{16}$$

Because the refractive index of extraordinary ray varies for different incident angle, according to the relationship between α and refractive index of extraordinary ray n_e in [43], we have

$$n_e = \frac{N_o N_e}{\sqrt{N_o^2 sin^2\alpha + N_e^2 cos^2\alpha}} = \frac{N_o N_e}{\sqrt{N_o^2 + (N_e^2 - N_o^2)cos^2\alpha}} \tag{17}$$

where N_o and N_e are principal refractive indices and are fixed for each type of material. According to (16),(17), we have:

$$n_e = \frac{N_o N_e}{\sqrt{N_o^2 + (N_e^2 - N_o^2)cos^2\gamma sin^2\theta_e}} \tag{18}$$

According to Snell's Law, we have:

$$n_{air} sin\theta = n_e sin\theta_e = n_o sin\theta_o \tag{19}$$

where $n_{air} \approx 1$ is the refractive index in air. Then we have

$$n_e = \frac{sin\theta}{sin\theta_e}. \tag{20}$$

According to (18),(20), we have:

$$\theta_e = \arcsin\sqrt{\frac{sin^2\theta}{N_e^2 - sin^2\theta(\frac{N_e^2}{N_o^2}cos^2\gamma - cos^2\gamma)}} \tag{21}$$

Finally, according to (20) and (21), we have:

$$n_e = \sqrt{N_e^2 - sin^2\theta(\frac{N_e^2}{N_o^2}cos^2\gamma - cos^2\gamma)} \tag{22}$$

Because the optical path difference is:

$$\Delta = d(n_e cos\theta_e - n_o cos\theta_o) \tag{23}$$

We substitute n_e, θ_e, and n_o, θ_o into Eq. 23, we can have expression of Δ using known parameters:

$$\Delta = d(\sqrt{N_e^2 - sin^2\theta(sin^2\gamma + \frac{N_e^2}{N_o^2}cos^2\gamma)} - \sqrt{N_o^2 - sin^2\theta}) \tag{24}$$

REFERENCES

[1] Swarun Kumar, Stephanie Gil, Dina Katabi, and Daniela Rus. Accurate indoor localization with zero start-up cost. In *Proceedings of ACM MobiCom*, 2014.

[2] Souvik Sen, Jeongkeun Lee, Kyu-Han Kim, and Paul Congdon. Avoiding multipath to revive inbuilding wifi localization. In *Proceedings of ACM MobiSys*, 2013.

[3] Jie Xiong and Kyle Jamieson. Arraytrack: a fine-grained indoor location system. In *Proceedings of USENIX NSDI*, 2013.

[4] Kiran Joshi, Steven Hong, and Sachin Katti. Pinpoint: Localizing interfering radios. In *Proceedings of USENIX NSDI*, 2013.

[5] Jon Gjengset, Jie Xiong, Graeme McPhillips, and Kyle Jamieson. Phaser: enabling phased array signal processing on commodity wifi access points. In *Proceedings of ACM MobiCom*, 2014.

[6] Fadel Adib, Hongzi Mao, Zachary Kabelac, Dina Katabi, and Robert C Miller. Smart homes that monitor breathing and heart rate. In *Proceedings of ACM CHI*, 2015.

[7] Fadel Adib, Zachary Kabelac, and Dina Katabi. Multi-person localization via rf body reflections. In *Proceedings of USENIX NSDI*, 2015.

[8] Fadel Adib, Zach Kabelac, Dina Katabi, and Robert C Miller. 3d tracking via body radio reflections. In *Proceedings of USENIX NSDI*, 2014.

[9] Yu-Lin Wei, Chang-Jung Huang, Hsin-Mu Tsai, and Kate Ching-Ju Lin. Celli: Indoor positioning using polarized sweeping light beams. In *Proceedings of ACM MobiSys*, 2017.

[10] Julian Randall, Oliver Amft, Jürgen Bohn, and Martin Burri. Luxtrace: indoor positioning using building illumination. *Personal and ubiquitous computing*, 11(6):417–428, 2007.

[11] Nishkam Ravi and Liviu Iftode. *Fiatlux: Fingerprinting rooms using light intensity*. na, 2007.

[12] Jean Armstrong, Y Sekercioglu, and Adrian Neild. Visible light positioning: a roadmap for international standardization. *IEEE Communications Magazine*, 51(12):68–73, 2013.

[13] Bo Xie, Kongyang Chen, Guang Tan, Mingming Lu, Yunhuai Liu, Jie Wu, and Tian He. Lips: A light intensity–based positioning system for indoor environments. *ACM Transactions on Sensor Networks*, 12(4):28, 2016.

[14] Radu Stoleru, Tian He, John A. Stankovic, and David Luebke. A high-accuracy, low-cost localization system for wireless sensor networks. In *Proceedings of ACM SenSys*, 2005.

[15] Bo Xie, Guang Tan, and Tian He. Spinlight: A high accuracy and robust light positioning system for indoor applications. In *Proceedings of ACM SenSys*, 2015.

[16] Song Liu and Tian He. Smartlight: Light-weight 3d indoor localization using a single led lamp. In *Proceedings of ACM SenSys*, 2017.

[17] Zhice Yang, Zeyu Wang, Jiansong Zhang, Chenyu Huang, and Qian Zhang. Wearables can afford: Light-weight indoor positioning with visible light. In *Proceedings of ACM MobiSys*, 2015.

[18] Chi Zhang and Xinyu Zhang. Litell: robust indoor localization using unmodified light fixtures. In *Proceedings of ACM MobiCom*, 2016.

[19] Chi Zhang and Xinyu Zhang. Pulsar: Towards ubiquitous visible light localization. In *Proceedings of ACM MobiCom*, 2017.

[20] Shilin Zhu and Xinyu Zhang. Enabling high-precision visible light localization in today's buildings. In *Proceedings of ACM MobiSys*, 2017.

[21] Masaki Yoshino, Shinichiro Haruyama, and Masao Nakagawa. High-accuracy positioning system using visible led lights and image sensor. In *Proceedings of IEEE RWS*, 2008.

[22] S-H Yang, E-M Jeong, D-R Kim, H-S Kim, Y-H Son, and S-K Han. Indoor three-dimensional location estimation based on led visible light communication. *Electronics Letters*, 49(1):54–56, 2013.

[23] Ye-Sheng Kuo, Pat Pannuto, Ko-Jen Hsiao, and Prabal Dutta. Luxapose: Indoor positioning with mobile phones and visible light. In *Proceedings of ACM MobiCom*, 2014.

[24] Ruipeng Gao, Yang Tian, Fan Ye, Guojie Luo, Kaigui Bian, Yizhou Wang, Tao Wang, and Xiaoming Li. Sextant: Towards ubiquitous indoor localization service by photo-taking of the environment. *IEEE Transactions on Mobile Computing*, 15(2):460–474, 2016.

[25] Edward Collett. *Field guide to polarization*, volume 15. SPIE press Bellingham, 2005.

[26] Wikipedia. Color wheel. https://en.wikipedia.org/wiki/Color_wheel#Color_wheels_and_paint_color_mixing.

[27] Zhao Tian, Yu-Lin Wei, Xi Xiong, Wei-Nin Chang, Hsin-Mu Tsai, Kate Ching-Ju Lin, Changxi Zheng, and Xia Zhou. Position: Augmenting inertial tracking with light. In *Proceedings of ACM VLCS*, 2017.

[28] Yuanqing Zheng, Guobin Shen, Liqun Li, Chunshui Zhao, Mo Li, Feng Zhao, Yuanqing Zheng, Guobin Shen, Liqun Li, Chunshui Zhao, et al. Travi-navi: Self-deployable indoor navigation system. *IEEE/ACM Transactions on Networking (TON)*, 25(5):2655–2669, 2017.

[29] Mei Wang, Zhehui Zhang, Xiaohua Tian, and Xinbing Wang. Temporal correlation of the rss improves accuracy of fingerprinting localization. In *INFOCOM 2016-The 35th Annual IEEE International Conference on Computer Communications, IEEE*, pages 1–9. IEEE, 2016.

[30] Jizhong Zhao, Wei Xi, Yuan He, Yunhao Liu, Xiang-Yang Li, Lufeng Mo, and Zheng Yang. Localization of wireless sensor networks in the wild: Pursuit of ranging quality. *IEEE/ACM Transactions on Networking (ToN)*, 21(1):311–323, 2013.

[31] Kun Qian, Chenshu Wu, Zheng Yang, Yunhao Liu, Fugui He, and Tianzhang Xing. Enabling contactless detection of moving humans with dynamic speeds using csi. *ACM Transactions on Embedded Computing Systems (TECS)*, 17(2):52, 2018.

[32] Zuwei Yin, Chenshu Wu, Zheng Yang, and Yunhao Liu. Peer-to-peer indoor navigation using smartphones. *IEEE Journal on Selected Areas in Communications*, 35(5):1141–1153, 2017.

[33] Kun Qian, Chenshu Wu, Yi Zhang, Guidong Zhang, Zheng Yang, and Yunhao Liu. Widar2. 0: Passive human tracking with a single wi-fi link. *Procs. of ACM MobiSys*, 2018.

[34] Chunyi Peng, Guobin Shen, and Yongguang Zhang. Beepbeep: A high-accuracy acoustic-based system for ranging and localization using cots devices. *ACM Transactions on Embedded Computing Systems*, 11(1):4:1–4:29, 2012.

[35] K. Liu, X. Liu, L. Xie, and X. Li. Towards accurate acoustic localization on a smartphone. In *Proceedings of IEEE INFOCOM*, 2013.

[36] K. Liu, Xinxin Liu, and Xiaolin Li. Acoustic ranging and communication via microphone channel. In *Proceedings of IEEE GLOBECOM*, 2012.

[37] K. Liu, X. Liu, and X. Li. Guoguo: Enabling fine-grained smartphone localization via acoustic anchors. *IEEE Transactions on Mobile Computing*, 15(5):1144–1156, 2016.

[38] R. Nandakumar, S. Gollakota, and N. Watson. Contactless sleep apnea detection on smartphones. In *Proceedings of ACM MobiSys*, 2015.

[39] Pengfei Zhou, Yuanqing Zheng, and Mo Li. How long to wait?: Predicting bus arrival time with mobile phone based participatory sensing. In *Proceedings of ACM MobiSys*, 2014.

[40] Yin Chen, Jie Liu, Dimitrios Lymberopoulos, and Bodhi and Priyantha. Fm-based indoor localization. In *Proceedings of ACM MobiSys*, 2012.

[41] Yonghang Jiang, Zhenjiang Li, and Jianping Wang. Ptrack: Enhancing the applicability of pedestrian tracking with wearables. *IEEE Transactions on Mobile Computing*, 2018.

[42] SHEN Wei-min. Interference pattern of convergent light for a uniaxial crystal with optical axis parallel to surface [j]. *College Physics*, 6:001, 2005.

[43] Dennis H Goldstein. *Polarized light*. CRC press, 2017.